Origami Inspired Soft Robotic Arm: A Modular Platform for Manipulation

Jiyang Wang[1], Yuchen You[1], Xinqi Zhang[1], Haobo Fang[1], Jiaqi Wang[2], Xiaonan Huang[2]

***Abstract*— Soft pneumatic robotic arms have recently emerged as promising alternatives to rigid manipulators due to their compliance, adaptability, and inherent safety. However, their deployment in space environments remains constrained by structural inflexibility, limited reconfigurability, and reliance on bulky external pneumatic sources. This work presents a lightweight, modular, and electronics-integrated soft robotic arm tailored for application scenarios that demand fault tolerance, adaptability, and robustness. The arm is composed of plug-and-play modules integrating 3D-printed Kresling origami actuators, proprioceptive sensing, and CAN-based communication, allowing dynamic adjustment of arm length and configuration to accommodate diverse operational scenarios. The embedded control architecture enables real-time trajectory tracking with an average relative error of 2.57% under multi-module configurations. Its modularity, versatility and repeatability offer key advantages for resilient and reconfigurable operation in future long-duration space missions, demonstrating strong potential for space robotics applications, particularly in autonomous inspection, maintenance, and sample collection in uncertain or low-gravity environments.**

I. INTRODUCTION

Robotic arms are versatile mechanical devices widely used in industrial automation, healthcare, and service robotics for tasks such as assembly, material handling, and inspection. In recent years, soft robotic arms have emerged as a promising alternative to traditional rigid manipulators, offering enhanced compliance, adaptability, and safety—features that are particularly advantageous in unstructured or dynamic environments. These characteristics have sparked growing interest in soft arms for field robotics, where environmental uncertainty and physical demands challenge conventional designs.

Such challenges are especially pronounced in space robotics, which imposes strict requirements on system weight, fault tolerance, reconfigurability, and autonomous operation in low-gravity or remote environments. However, current soft robotic arms often struggle to meet these demands due to their reliance on bulky external pneumatic systems, limited modularity, and poor controllability outside laboratory conditions [1], [2]. These limitations restrict their practical deployment in space-related tasks such as infrastructure maintenance, on-orbit inspection, and extraterrestrial sample collection. Addressing these gaps calls for the development of new soft robotic architectures that integrate lightweight construction, embedded electronics, and modular design to achieve robust and flexible performance across a wide range of challenging application scenarios—including those beyond Earth.

Building upon these motivations, we present a modular soft robotic arm composed of 3D-printed Kresling origami actuators, integrated with embedded sensing and actuation electronics. The arm is constructed from plug-and-play modules that allow rapid reconfiguration, enabling flexible adaptation to diverse manipulation tasks. A unified CAN bus architecture facilitates both communication and sensing, supporting synchronized control and distributed proprioception across dynamically changing hardware configurations. This design ensures reliable real-time tracking performance while maintaining resilience against component failures and mission drift—critical features for operation in unpredictable environments.

Our approach couples mechanical simplicity with a robust control framework grounded in piecewise constant curvature (PCC) kinematics and Jacobian-based redundancy resolution, which enables precise and flexible motion control despite the inherent compliance and redundancy of soft structures. Together, these elements establish a promising platform not only for terrestrial field applications but also for future long-duration space missions that demand reusability, adaptability, and safe physical interaction across uncertain and resource-constrained environments.

II. METHODOLOGY

A. Mechanical Design

By integrating compact actuation mechanisms, embedded proprioception, and modular quick-assembly interfaces, each arm module functions as an independent unit capable of self-sensing and rapid deployment, providing a robust foundation for scalable, reconfigurable, and autonomous soft robotic systems.

Each arm module is composed of three Kresling origami actuators arranged in parallel to form a tripod-like configuration. This arrangement introduces additional degrees of freedom (DoF), enabling coordinated multi-axis movements and a broad workspace in three dimensions (Fig. 1). Kresling origami was selected as the actuator for each module due to its high contraction ratio and its inherent ability to twist while contracting, offering a compact and efficient means of generating complex motions from simple structural deformations [3].

To facilitate deformation proprioception, a diametrically magnetized magnet is embedded at the tip of every origami

[1] Jiyang Wang, Yuchen You, Xinqi Zhang, and Haobo Fang are with the EECS Department, University of Michigan, Ann Arbor, MI, USA
realwjy, yuchenxr, dadaaa, fanghb@umich.edu
[2] Jiaqi Wang and Xiaonan Huang are with the Robotics Department, University of Michigan, Ann Arbor, MI, USA
wangjq, xiaonanh@umich.edu

unit. Paired with magnetic encoders, this setup allows real-time proprioceptive feedback of the actuator's twisting motion, forming the basis for closed-loop deformation control. Pneumatic actuation is applied individually to each origami chamber, and due to the symmetric geometry, force is distributed evenly across the actuators, resulting in smooth and consistent deformation behavior. This uniformity simplifies control and improves motion repeatability across a variety of operating conditions.

To further support field or space deployment, a custom-designed quick-assembly, quick-release mechanical interface is implemented at both ends of each module, as shown in 1. The proper alignment of embedded pneumatic and electrical interfaces allows hot-swapping of faulty units and seamless expansion or adaptation of the arm's configuration to meet task-specific needs. These features enable fast and secure mechanical coupling between modules without requiring specialized tools, significantly reducing the time and effort needed for system reconfiguration, replacement, or maintenance.

Moreover, all pneumatic channels and electronic wiring are embedded within the 3D-printed outer shells of the modules. This integrated design eliminates the need for external tubing or cabling, reducing the risk of mechanical entanglement or damage during operation while enhancing the system's structural robustness and compactness. By minimizing external components, the arm is well-suited for deployment in cluttered, dynamic, or low-gravity environments where reliability and space efficiency are critical. A complete view of the assembled arm and detailed module breakdown are shown in Fig. 1, illustrating the system's integration, modularity, and elegant design.

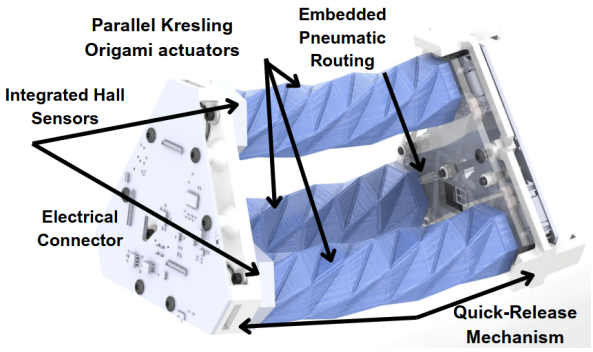

Fig. 1. Modular design featuring a quick-release mechanism for rapid assembly and disassembly, embedded pneumatic and electric routing reducing the number of external tubing or cabling, and parallel Kresling origami to enable multi-axis motion with enhanced structural stability and a compact form factor.

B. Electrical System

Two custom-designed printed circuit boards (PCBs) are integrated at each end of every origami module to enable localized sensing and actuation. As shown in Fig. 2, each module incorporates a sensing board and an actuation board, both connected via a CAN bus for synchronized communication. The sensing board features three Hall-effect rotary encoders (AS5600; ams OSRAM) to measure actuator rotation angles, along with an inertial measurement unit (IMU, BNO055; Bosch Sensortec) that enhances state estimation accuracy during dynamic motion by compensating for errors in the actuator length reconstruction.

On the actuation side (Fig. 3), each board is equipped with three pairs of solenoid valves (X-Valve; Parker), one two-way and one three-way per actuator, to control the pneumatic flow. A closed-loop PID controller regulates each actuator's length in real time. The primary actuation board in the system integrates an OrangePi CM5, responsible for motion planning and complex computational tasks such as kinematics and trajectory generation. Subsequent actuation boards adopt a microcontroller (STM32G431CBU6; ST) for localized valve control and lower-level signal processing. The CAN bus enables robust, scalable communication between all modules, allowing for synchronized multi-module operation and easy system expansion. This distributed architecture supports modularity and reconfigurability while maintaining reliable control performance across a range of tasks.

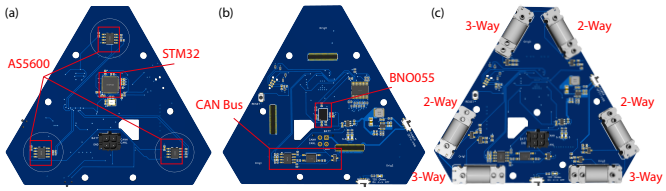

Fig. 2. Layouts showing the PCB designs. (a) and (b) show the top and bottom view of the sensing board with multiple integrated sensors. (c) shows the actuation board installed with solenoid valves.

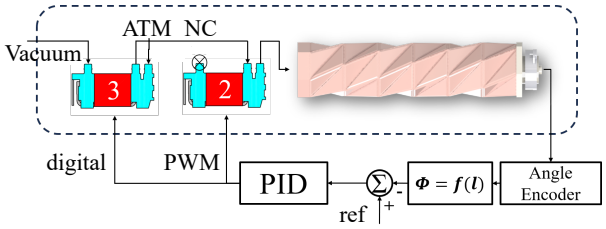

Fig. 3. A diagram showing how each actuator is controlled by a closed-loop system through angle encoders and valves.

C. Module's Geometric Model and Control

For the forward and inverse kinematics calculations, the target position is initially defined in the Cartesian coordinate space $(\hat{i}, \hat{j}, \hat{k})$. To map this position to the actuation space, it must first be transformed into the configuration space, denoted as Q_k [4].

In this work, we adopted the *Piecewise Constant Curvature (PCC) Assumption*, where each module's three origami-inspired structures are modeled as smooth curves with a constant curvature κ_{kj}. The end position of each module can then be expressed in the configuration space using the parameters $(\kappa_{kj}, \phi_k, \beta_k)$. Subsequently, to transform Q_k into the actuation space L_k, it is necessary to calculate

the transformation function f_2, which can be described as follows:

$$(x, y, z) \xleftarrow{f_1} (\kappa, \phi, \beta) \xleftarrow{f_2} (l_1, l_2, l_3) \tag{1}$$

Building on the single-section formulation, we extended our approach to a multi-section system. The Jacobian matrix J, which maps from the actuation space to the Cartesian coordinate space, was employed to address the redundancy inherent in our design, where multiple actuation solutions can achieve the same target configuration. To resolve this redundancy, we formulated the following least-squares optimization problem:

$$\arg\min_{\Delta l} \|J\Delta l - k_p \vec{e}_p\| + \lambda^2 \|\Delta l\|^2 ,$$

where J denotes the relevant portion of the Jacobian, k_p is a proportional gain, $\vec{e}_p$ is the position error, and λ is a regularization parameter that penalizes large actuation changes. Finally, we implemented a feedback control framework to enact the desired actuation, as illustrated in Fig.3.

III. Results

A. Evaluation of Motion Accuracy

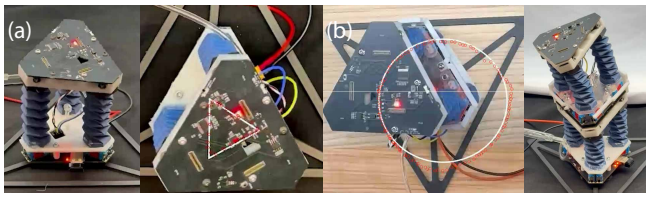

Fig. 4. Figures showing (a) a single soft arm module and (b) two connected soft arm modules tracking a triangular and a circular trajectory, respectively. The white curves indicate the target trajectories, while the red curves represent the actual trajectories.

Two groups of experiments were conducted to evaluate the arm's ability to track predefined trajectories under both single-module and dual-module configurations, as shown in Fig. 4. The experiments focused on assessing the system's motion accuracy and stability in performing typical planar trajectories. Tracker (Open Source Physics) was used to extract the actual end-effector trajectories from video recordings, while MATLAB was employed to compute the relative tracking errors between the commanded and actual paths.

In the single-module configuration (Fig. 4(a)), the soft arm demonstrated precise motion control when executing circular, triangular, and square trajectories. The system achieved an average relative error of 2.34%, with the maximum error reaching 7.30%. These results highlight the effectiveness of the PCC-based kinematic model and the reliability of the embedded sensing-feedback loop.

When extended to the dual-module configuration (Fig. 4(b)), the reachable workspace significantly increased, enabling more complex and larger-scale motions. Despite the higher control complexity introduced by the additional degrees of freedom, the system maintained a strong level of accuracy, achieving an average tracking error of 2.57% and a maximum error of 9.08% on a circular path. These results underscore the architecture's resilience, demonstrating that high tracking performance can be retained even in multi-module configurations.

B. Validation of Task Robustness

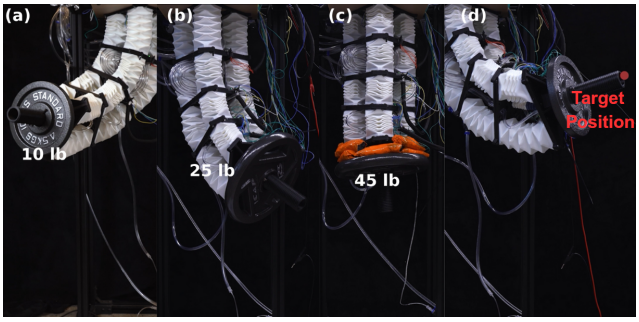

Fig. 5. Figures showing (a) the soft arm lifting a 10 lb payload, (b) the soft arm lifting a 25 lb payload, and (c) the soft arm lifting a 45 lb payload. (d) verifies the repeatability of the arm's performance under repeated actuation.

To further validate the robustness and scalability of the proposed modular system, we conducted a second set of experiments focused on payload capacity, structural resilience, and operational repeatability, as shown in Fig. 5. For high-payload applications, the three compact parallel Kresling origami actuators are replaced with three larger parallel Yoshimura origami actuators, while maintaining the same tripod configuration. Beyond that, a single Kresling origami with an integrated Hall sensor is positioned at the center to monitor the central axis length in real time. The soft robotic arm, assembled in its dual-module configuration, was tasked with lifting progressively heavier loads of 10 lb (4.5 kg), 25 lb (11.3 kg), and 45 lb (20.4 kg), significantly exceeding the actuator's own weight. These trials demonstrate not only the system's high payload-to-weight ratio, but also its structural integrity under demanding load conditions.

The ability to lift a 45 lb payload, as shown in Fig. 5(c), represents a payload-to-mass ratio exceeding 2.5:1, highlighting the exceptional force amplification enabled by the embedded pneumatic actuation and the structurally efficient origami architecture. In addition, the system maintained stable behavior and showed no signs of structural failure or control degradation throughout all trials, underscoring its resilience and suitability for high-force tasks.

In addition to payload capacity, we evaluated the system's repeatability by subjecting it to repeated actuation cycles while tracking end-effector positioning (Fig. 5(d)). The arm consistently returned to the target position within a positional tolerance of ±10 mm, confirming reliable performance over time. This level of repeatability, achieved with minimal sensor drift or mechanical fatigue, affirms the viability of the arm for tasks requiring high consistency in both terrestrial and space-based applications.

In general, these results demonstrate the soft arm's mechanical robustness, reliable control performance, and scalable architecture capable of adapting to varying task demands

through rapid module addition or replacement. Such versatility is essential for autonomous operations in complex and resource-constrained space environments, where adaptability and resilience are critical for long-term deployment.

IV. Future Work

Future research will focus on developing onboard decision-making algorithms to enhance the arm's autonomy and versatility. Further improvements in control are also needed to increase stability during high-load or extended-reach operations. In addition, integrating a camera and a range of end-effectors will expand the potential of the arm for diverse applications.

References

[1] Y. Zhang, X. Li, P. Wang, Q. Chen, and Y. Liu, "A tendon-driven continuum manipulator with robust shape estimation by multiple imus," *IEEE Robotics and Automation Letters*, vol. 8, no. 2, pp. 1234–1241, 2023.

[2] S. Ku, B.-H. Song, T. Park, Y. Lee, and Y.-L. Park, "Soft modularized robotic arm for safe human–robot interaction based on visual and proprioceptive feedback," *The International Journal of Robotics Research*, vol. 43, no. 8, pp. 1128–1150, 2024.

[3] W. Fan, J. Wang, Z. Zhang, G. Chen, and H. Wang, "Vacuum-driven parallel continuum robots with self-sensing origami linkages," *IEEE/ASME Transactions on Mechatronics*, vol. 29, no. 5, pp. 3370–3380, 2024.

[4] B. Jones and I. Walker, "Kinematics for multisection continuum robots," *IEEE Transactions on Robotics*, vol. 22, no. 1, pp. 43–55, 2006.